Quantifying the magnitude and spatial variability of bedrock erosion beneath the Sisters Glacier, Washington using cosmogenic ^{3}He concentrations

Sarah Francis[1], Doug Clark[1], Ken Farley[2], Colin Amos[1], Paul Bierman[3]

1. Western Washington University, Bellingham, WA; 2. California Institute of Technology, Pasadena, CA; 3. University of Vermont, Burlington, VT.

Introduction

Cirque glaciers are common in temperate mountains around the world, and thereby a dominant agent of erosion in these high mountain settings (e.g., Anderson, 1978; Larsen and Mangerud, 1981; National Snow and Ice Data Center, 2017). The processes and rates of this erosion, however, are not well-understood (Koppes et al., 2015). Current understanding of cirque-glacial erosion rates and mechanisms is limited. Published values for cirque-glacial erosion rates are rare and highly variable (0.008-10 mm/yr), and mostly rely on indirect estimates from sediment volumes (e.g., Sanders et al., 2013; Herman et al., 2015) or theoretical models (Iverson, 2012); Anderson, 2014). ^{3}He cosmogenic nuclide analyses provide a tool to infer cirque-glacial erosion depths at a relatively high spatial resolution (Briner and Swanson, 1998: Crest et al., 2017). ^{3}He accumulates in bedrock exposed at the surface as a result of cosmic ray bombardment. The concentration of cosmogenic ^{3}He increases with exposure time as well as proximity to the surface (Gosse and Phillips, 2001). With an independent estimate of surface exposure age, cosmogenic ^{3}He concentrations can be used to infer erosion depths on glaciated bedrock surfaces (**Figure 1**). The spatial variability of erosion can be used to infer mechanisms of erosion. Spatially variable erosion indicates a plucking-dominant environment, whereas spatially consistent and decreasing downslope indicates an abrasion-dominated environment (**Figure 2**).

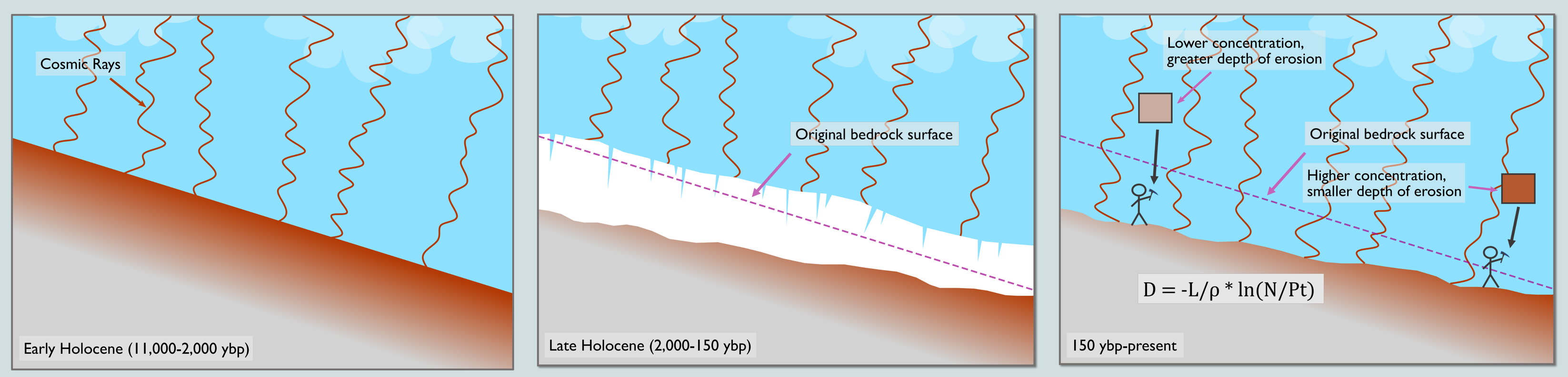

Figure 1: Cartoon cross-section schematic showing how cosmogenic ^{3}He measurements are used to calculate glacial erosion depth with a known surface exposure age in the Twin Sisters. In the early Holocene, cosmic rays produce cosmogenic ^{3}He in bedrock at a consistent rate. Production decreases with depth. In the late Holocene, the overriding glacier blocks cosmic rays and erodes away at bedrock with accumulated cosmogenic ^{3}He. At present, cosmogenic ^{3}He concentrations (*N*) are measured in bedrock samples and depth of glacial erosion (*d*) is calculated with the equation shown, where *L* is attenuation length (a physical constant), *ρ* is rock density, *P* is production rate of cosmogenic ^{3}He, and *t* is period of exposure time.

Study Location

The Sisters Glacier is located in the Twin Sisters Range, North Cascades, Washington and is composed entirely of ultramafic dunite (~93% olivine) bedrock (Christensen, 1971; **Figure 3**). The range is part of the North Cascades, which extend from central Washington State wo southwestern British Columbia. The Twin Sisters Range is an ideal location for this type of study because cosmogenic ^{3}He is produced rapidly in olivine and can be measured after relatively short periods of surface exposure (<1,000 years; Kurz and Brook, 1994). Detailed Holocene glacial chronologies from nearby Mount Baker indicate that the Holocene forefield of the Sisters Glacier was likely exposed around 11,000 years ago following Pleistocene deglaciation, exposed to cosmic rays for 9,000 years, and then covered by Neoglacial ice for 2,000 years until the last century (**Figure 1**, Clague et al., 1997; Kovanen and Easterbrook, 2001; Menounos et al., 2009; Osborn et al., 2012). This detailed proxy record of Holocene glacier extents for the Sisters Glacier provides a crucial constraint on timing of Holocene glaciation necessary to estimate rates of erosion beneath the glacier.

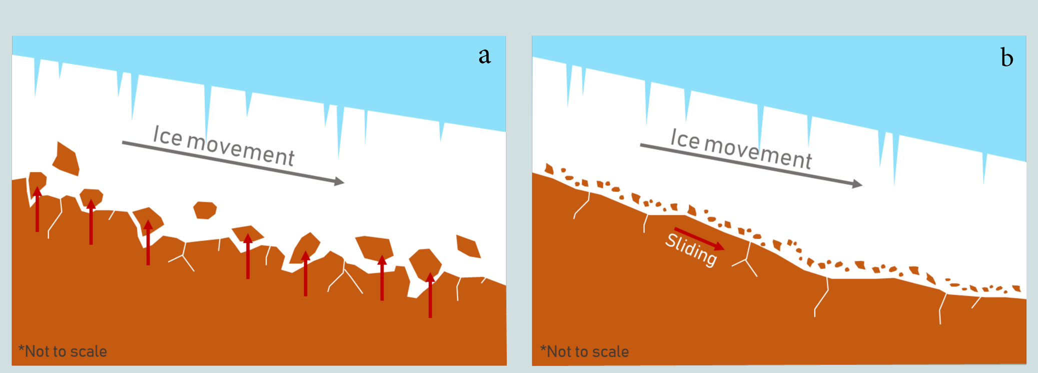

Figure 2: Cartoon cross-sections of theoretical mechanisms of glacial erosion. Plucking (a) is a process where glacial ice removes large blocks of rock all at once (usually taking advantage of existing fractures), and abrasion (b) is a process where small grains embedded in the base of the glacier scrape at the bedrock surface.

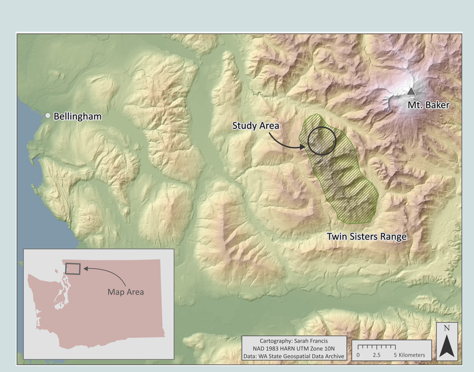

Figure 3: Location of Twin Sisters Range within the state of Washington. Green shaded area shows extent of dunite body, and study area shown in grey circle.

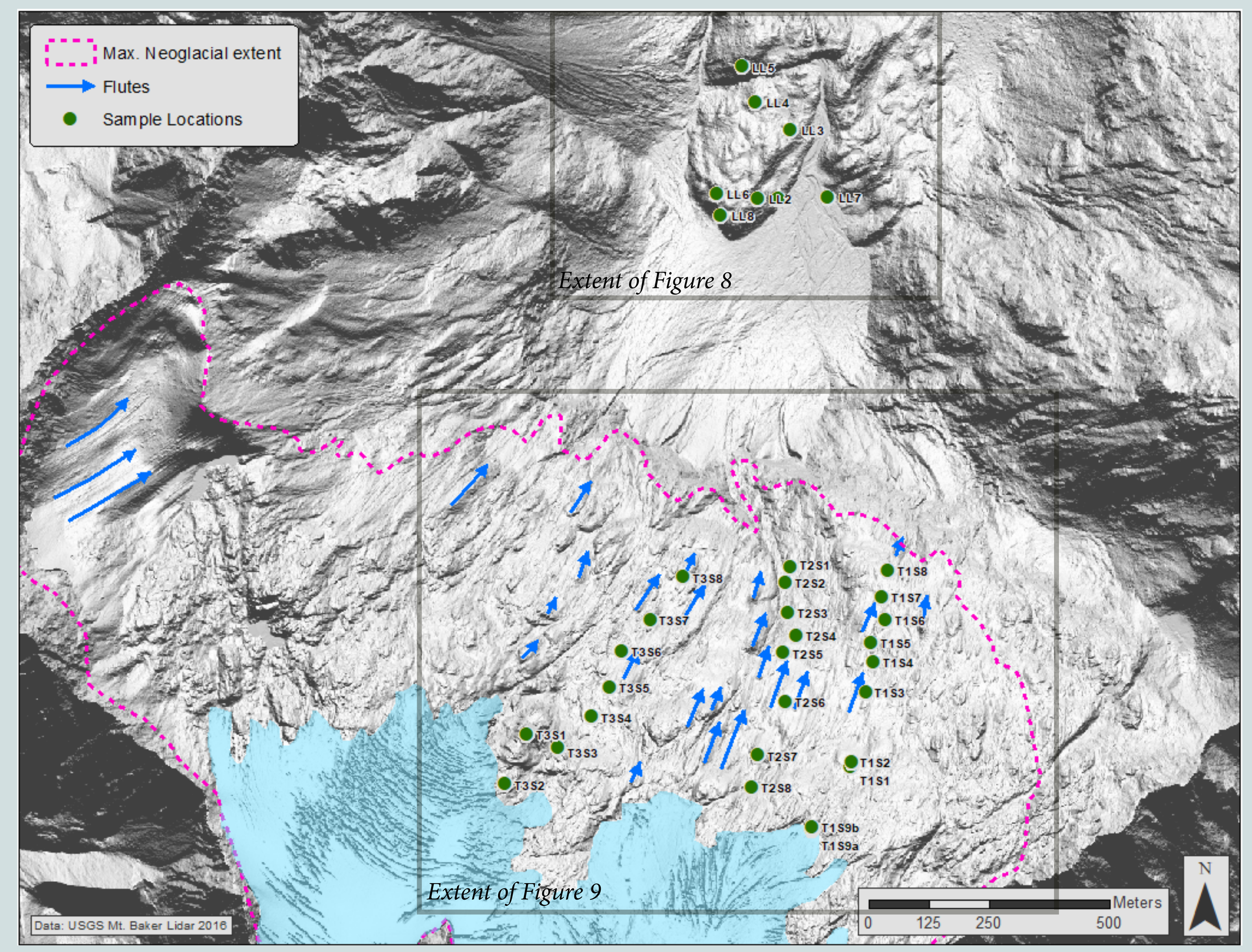

Figure 4: Lidar hillshade of Sisters Glacier, mapped Neoglacial maximum, glacial flutes, and lowland and forefield sample locations.

Methods

- Field mapping, lidar data, and aerial imagery were to identify bedrock fractures, glacial fluting, historic glacial extents, and terminal moraines in the forefield of the Sisters Glacier: used to establish the Holocene maximum glacial extent (**Figure 4**).
- Bedrock samples were collected along glacial flow-line transects in the forefield (**Figure 4**), and cosmogenic ^{3}He concentrations were measured in these samples to estimate Holocene cirque-glacial erosion depths.
- Cosmogenic ^{3}He was measured in several "lowland" sites outside the extent of Holocene glaciation to test if warm-based Pleistocene glaciation eroded enough material to remove cosmogenic ^{3}He from prior exposure (**Figure 4**).
- Standard crushing methods to remove mantle-sourced ^{3}He were not successful in dunite rock; we thus calculated cosmogenic component based on ^{3}He/^{4}He ratios in shielded samples (1.8-2.8 R_A) collected from a nearby quarry (**Figure 5**).

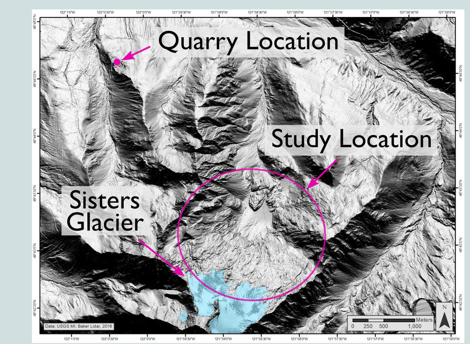

Figure 5: Lidar hillshade of Sisters Glacier, study area, and quarry location.

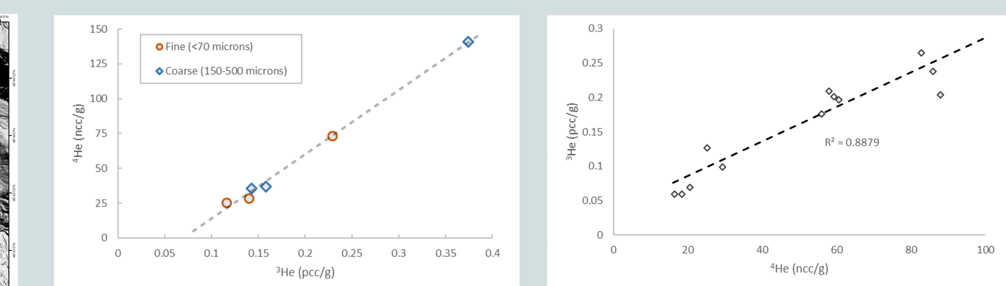

Figure 6 (left): ^{3}He/^{4}He scatter plot of exposed samples results processed at two different grain size fractions. Figure 7 (right): ^{3}He/^{4}He scatter plot of shielded samples from quarry. This plot constrains the mantle ^{3}He/^{4}He ratio.

Results and Conclusions

We were unable to remove mantle-sourced ^{3}He from our samples with conventional crushing methods; analyzing different grain size fractions of several exposed samples had no significant effect on ^{3}He concentrations (**Figure 6**). However, all shielded samples showed air-normalized ^{3}He/^{4}He ratios of 1.69-3.72 R_A, with an average of 2.3 R_A (r^2=0.89, **Figure 7**). Our analyses of lowland samples show two exposure ages older than expected, two younger, and two approximately consistent with late-Pleistocene deglaciation (**Figure 8**). This suggests that Pleistocene deglaciation did not remove all cosmogenic ^{3}He from prior exposure in all samples, and that some samples had unaccounted for shielding. However, similar cosmogenic inheritance is unlikely in forefield samples because none of the samples have model exposure ages older than 11,000 yrs. Our analyses of forefield samples show decreasing model exposure ages (10,500-0 yrs) and concomitant increasing depths of erosion (0.15-146 cm) with proximity to the modern glacier (**Figure 9**). Patterns in erosion rates are less clear due to larger uncertainties, but potentially show increasing rates of subglacial erosion (0.001-0.7 mm/yr) with proximity to the modern glacier (**Figure 9**). The relatively low magnitudes and consistent patterns of erosion suggest that abrasion and/or small plucking events (centimeters to decimeters) are the dominant mechanisms of erosion underneath the Sisters Glacier.

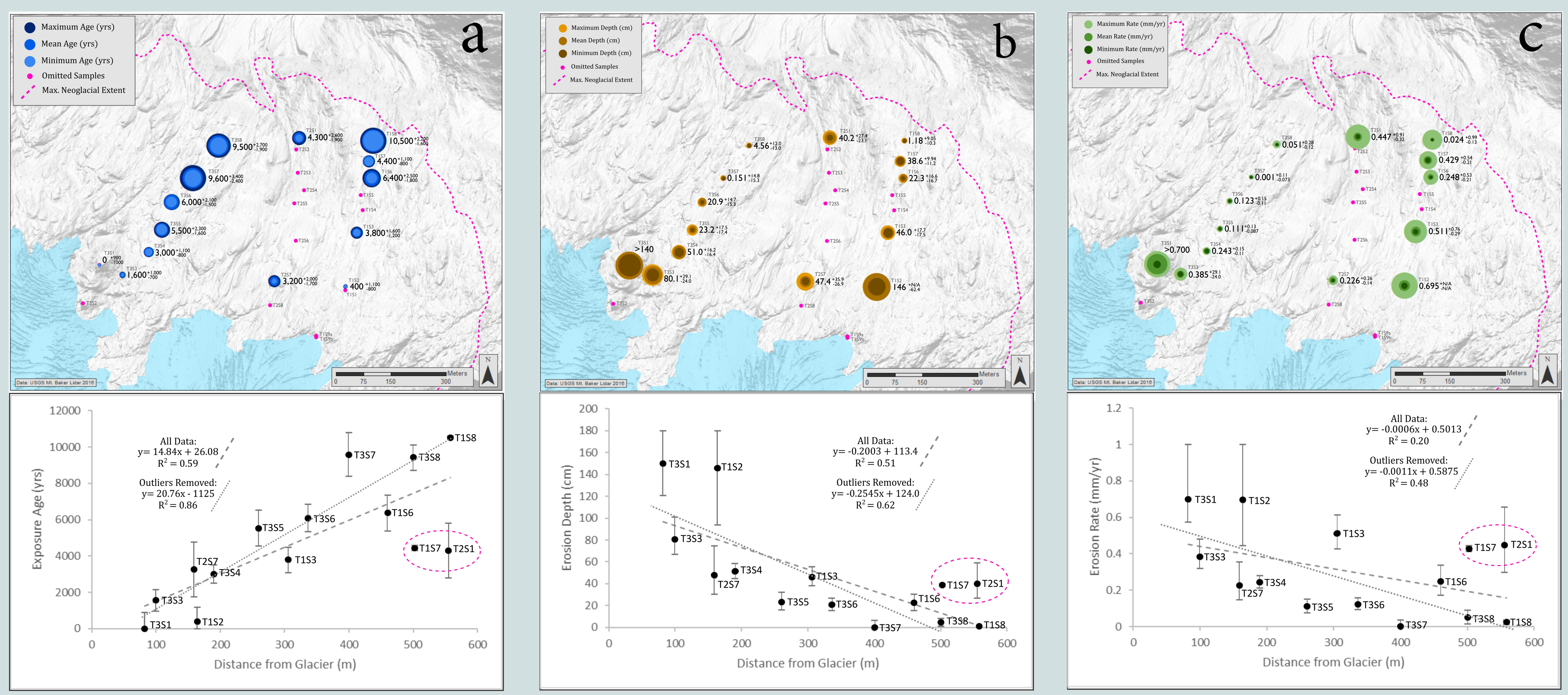

Figure 9: Results of forefield analyses showing exposure ages (a), erosion depths (b), and erosion rates (c). Map view shows uncertainties related to snow shielding, period of glaciation, and mantle ^{3}He/^{4}He ratio. Plots show values relative to distance from the modern glacier, with uncertainties related to mantle ^{3}He/^{4}He ratio only. Trendlines and r-squared values are shown with and without outliers (circled in plot).

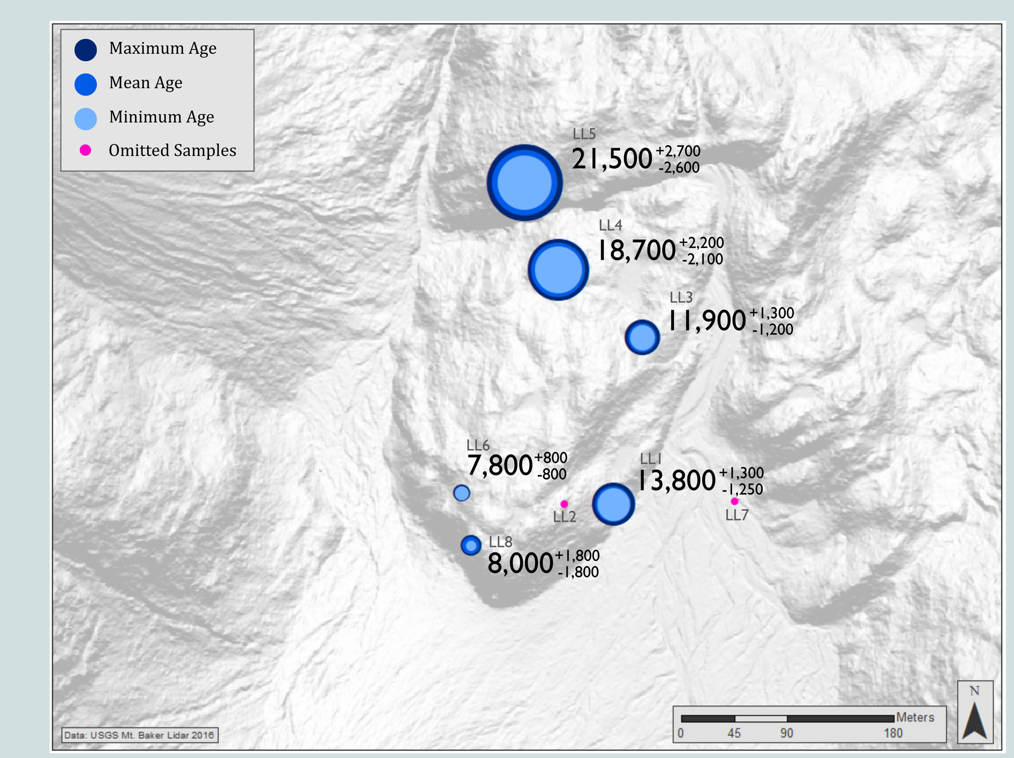

Figure 8: Lowland sample sites and exposure ages, including uncertainties related to snow shielding and ^{3}He/^{4}He ratios. Omitted analyses rejected based on high ^{4}He concentrations.

Acknowledgements: Thank you to the Northwest Scientific Association, the Geological Society of America, Western Washington University Graduate School, Western Washington University Department of Geology, Caltech, and Weyerhaeuser for making this research possible.

For more information about this research, please contact Sarah Francis at *francis3@wwu.edu*.

References

Anderson, 1978, Cirque Glacier Erosion Rates and Characteristics of Neoglacial Tills, Pangnirtung Fiord Area, Baffin Island, NWT, Canada: Arctic and Alpine Research, v. 10, p. 749.

Anderson, 2014, Evolution of lumpy glacial landscapes: Geology, v. 42, p. 679-682.

Briner and Swanson, 1998, Using inherited cosmogenic 36Cl to constrain glacial erosion rates of the Cordilleran ice sheet: Geology, v. 26, p. 3.

Christensen, 1971, Fabric, Seismic Anisotropy, and Tectonic History of the Twin Sisters Dunite, Washington: Geological Society of America Bulletin, v. 82, p. 1681-1694.

Clague et al., 1997, Pre-Younger Dryas resurgence of the southwestern margin of the Cordilleran ice sheet, British Columbia, Canada: Boreas, v. 26, p. 261-278.

Crest et al., 2017, Cirques have growth spurts during deglacial and interglacial periods: Evidence from 10Be and 26Al nuclide inventories in the central and eastern Pyrenees: Geomorphology, v. 278, p.60-77.

Gosse and Phillips, 2001, Terrestrial in situ cosmogenic nuclides: theory and application: Quaternary Science Reviews, v. 20, p. 1475-1560.

Herman et al., *2015*, Erosion by an Alpine glacier: Science, v. 350, p.193-195.

Iverson, 2012, A theory of glacial quarrying for landscape evolution models: Geology, v. 40, p. 679-682.

Koppes et al., 2015, Observed latitudinal variations in erosion as a function of glacier dynamics: Nature, v. 526, p. 100-103.

Kovanen and Easterbrook, 2001, Late Pleistocene, post-Vashon, alpine glaciation of the Nooksack drainage, North Cascades, Washington: Geological Society of America Bulletin, v. 113, p. 274-288.

Kurz and Brook, 1994, Surface Exposure Dating with Cosmogenic Nuclides, in Dating in Exposed and Surface Contexts, Albuquerque, University of New Mexico Press, p. 139-159.

Larsen and Mangerud, 1981, Erosion Rate of a Younger Dryas Cirque Glacier at Krakenes, Western Norway: Annals of Glaciology, v. 2, p. 153-158.

Menounos et al., 2009, Latest Pleistocene and Holocene glacier fluctuations in western Canada: Quaternary Science Reviews, v. 28, p. 2049-2074.

National Snow and Ice Data Center, 2017, "About Glaciers": accessed May 2017.

Osborn et al., 2012, Latest Pleistocene and Holocene glacier fluctuations on Mount Baker, Washington: Quaternary Science Reviews, v. 49, p. 33-51.

Sanders et al., 2013, The sediment budget of an alpine cirque: Geological Society of America Bulletin, v. 125, p. 229-248.